Energy and Fuels, Volume 33, Issue 8, 2019, pp. 7550-7560
DOI: 10.1021/acs.energyfuels.9b01256

CO_2 capture performance of gluconic acid-modified limestone-dolomite mixtures under realistic conditions

Ke Wang[1,2], Feng Gu[1], Peter T. Clough[2], Pengfei Zhao[1], Edward J. Anthony[2*]

[1] School of Electrical and Power Engineering, China University of Mining and Technology, Xuzhou 221116, China.

[2] Energy and Power Theme, Cranfield University, Cranfield, Bedfordshire, MK43 0AL, UK.

Ke Wang is currently a visiting professor at Cranfield University.

* Corresponding author: Edward J. Anthony, E: b.j.anthony@cranfield.ac.uk, T: +44 (0) 1234 752 823

Abstract: Calcium Looping (CaL) technology is potentially one of the more attractive ways to capture CO_2 from fossil fuel power plants. However, with increasing numbers of reaction cycles, the CO_2 capture capacity rapidly decreases. To address this shortcoming, limestone-dolomite mixtures reacted with gluconic acid to form Ca-Mg gluconics were explored to prepare highly effective, MgO-stabilized, CaO sorbents that exhibited a high and stable CO_2 capture capacity over multiple cycles. The sorbents were all tested over 10 carbonation-calcination cycles, under realistic CaL conditions (calcination in a high CO_2 concentration). The results indicate the development of an effective homogeneous composition between CaO and MgO – due to the small CaO crystallite size, porous texture, nanosheet (~100 nm thick) morphology. This provides sufficient void space for the volume expansion during carbonation to mitigate the effects of repeated cycle sintering and retain structural

stability. Here, MgO content as low as 10 mol% was able to ensure a superior CO_2 capture performance with a fast carbonation rate, high CO_2 carrying capacities and remarkable stability. Furthermore, these sorbents retained a conversion (above 90%) over multiple cycles following a recarbonation step.

1. Introduction

The 2015 United Nations Climate Change Conference (COP 21) committed the participating countries to limit global-mean temperature rise to well below 2 °C.[1] Such a challenging target is possible, but requires radical social and economic change, which include the use of carbon capture and storage to balance renewable power intermittency and decarbonization of heavy industries.[2] Here, the Calcium Looping (CaL) process has gained increasing profile[3-5] due to its advantages such as (i) use of inexpensive and widely available natural CaO precursors (i.e., limestone and dolomite), (ii) the high potential CO_2 capacity (~0.78 $gCO_2/gCaO$), (iii) the fast kinetics of carbonation and release reaction, and (iv) the potential market for used sorbents in the lime and cement industries: [6, 7]

$$CaO_{(s)} + CO_{2(g)} \rightleftarrows CaCO_{3(s)} \qquad \Delta H_r = -178 \text{ kJ mol}^{-1} \quad (1)$$

For CaL, flue gas containing ~15 vol% CO_2 in the case of coal-fired power stations is used to fluidize CaO-based particles in a carbonator under atmospheric pressure, where rapid carbonation of the sorbents occurs at temperatures around 650 °C.[8, 9] The carbonated particles are then transferred to another fluidized bed reactor where calcination of the sorbents takes place under high CO_2 partial pressure (70-90 vol%) at much higher temperatures (~950 °C).[10] The regeneration stage

requires oxy-fuel combustion, the use of high temperature steam or indirect heating of the reactor to generate a concentrated CO_2 gas stream for storage or utilization.[11]

Most limestone based sorbents studied so far, are able to achieve a high CO_2 uptake capacity in the first cycle, close to 100%.[12, 13] However, they suffer a progressive loss of CO_2 uptake capacity over increasing numbers of carbonation/calcination cycles.[14, 15] This poor cyclic stability is associated with a drastically reduced CaO surface area caused by sintering, since the harsh carbonation/calcination temperatures are well above the Tammann temperature (T_T) of $CaCO_3$ (~533 °C).[13, 16] A number of thermal/chemical treatments, including hydration[17, 18], self-reactivation[19, 20], re-carbonation[21, 22], doping[23], biomass templating[24-27] and acidification[28, 29] have been investigated to increase the porosity of the calcined material and in turn, reduce the deterioration of the sorbent. Unfortunately, these modified materials can still suffer from a significant deterioration in microstructure, in the absence of a structural stabilizer. Consequently, a number of microstructure stabilizers have been developed for incorporation into limestone based sorbents to reduce the loss of activity over multiple CaL cycles. [30, 31]

Natural dolomite ($CaMg(CO_3)_2$) has been examined as an alternative CaO precursor.[32] Compared with limestone-derived sorbents, dolomite based sorbents exhibit a reduced loss in CO_2 capture efficiency despite having a lower theoretical maximum CO_2 uptake capacity per unit mass of the sorbent, due to the fact that while the MgO component stabilizes the CaO grains and minimizes sintering, it itself does not capture CO_2.[12] The decomposition of $MgCO_3$ generates additional surface area

and pore volume, making reaction with CO_2 occur more easily.[33] Furthermore, the presence of MgO, which itself has a high-T_T of 1276 °C, serves as structural stabilizer to control sintering and maintain the sorbent morphology.[34] In addition, MgO is potentially a more preferable stabilizer for CaO, since MgO does not consume active CaO unlike Al_2O_3 or ZrO_2, which produce $Ca_xAl_yO_z$ and $CaZrO_3$ respectively.[35] A number of studies have attempted to employ treated/synthetic dolomite-based materials. Thus,Wang et al.[36] and Sánchez-Jiménez et al.[37] reported that dry ball-milling slightly enhanced the cyclic conversion of dolomite-derived sorbents. While, Sayyah[38], Kurlov et al.[39] and Sun et al.[40] found that wet ball-milled dolomite considerably improved the cyclic performance of the sorbent. In addition, an acid treatment approach has received increasing attention, thus Li et al.[29] treated dolomite with acetic acid and Wang et al.[41] treated dolomite with citric acid and further coupled this with a carbon coating to promote the CO_2 conversion of the sorbent. During mild calcination conditions, most of these treated dolomite-based materials exhibited an increased cyclic performance. However, Miranda-Pizarro et al.[42] recently demonstrated that acetic acid treatment of dolomite did not result in any improvement under realistic CaL conditions.

By contrast, treatment of limestone-dolomite mixtures has rarely been examined, previous studies with acid treatment were mainly focused on a rather limited choice of organic acids (acetic acid and citric acid). Also, past work usually involved testing the sorbents under mild calcination conditions (i.e. unrealistic low CO_2 concentrations in the calcination stage), leading to overly favorable results. [43]

Here, limestone-dolomite mixtures were reacted with several acids to prepare effective MgO-stabilized CaO sorbents. A relatively low amount of MgO (mole ratio of Mg/Ca = 1:9) was uniformly incorporated into CaO grains through a simple acid treatment process. Compared with other synthetic MgO-stabilized CaO materials, this approach is cheaper and more environmentally friendly procedure using natural limestone-dolomite mixtures as raw materials to enhance the long term carrying capacity even under harsh calcination conditions. In this work, the cyclic tests were performed under high CO_2 partial pressures during calcination conditions to demonstrate the practical ability of these sorbents. In addition, morphological characterization using a variety of techniques was used to gain an understanding of the fundamental mechanisms responsible for the improved CO_2 capture capacity and multi-cycle stability.

2. Experimental

2.1 Materials

Naturally occurring limestone ($CaCO_3$ with ~1 wt% impurities) was obtained from Tianjin, China. The dolomite (CaO 37.01 %, MgO 22.50 %, SiO_2 0.11 %, Fe_2O_3 0.10 %, and CO_2 balance) was obtained from Anhui Province, China. Organic acids, D-Gluconic acid solution (49-53 wt%), citric acid monohydrate (99.5 wt%), and glacial acetic acid (~97.0 wt%) were all obtained from Shanghai Aladdin Reagent Co., China.

2.2 Sorbents

Limestone, dolomite and limestone-dolomite mixtures were reacted with organic acid to prepare CaO-based sorbents using the following procedure. Firstly, the organic

acid (citric acid, anhydrous acetic acid, or gluconic acid) was dissolved in distilled water to form an acid solution. Then, a calculated amount of CaO precursor (limestone, dolomite, and limestone-dolomite mixtures with the molar ratio of Ca^{2+} to Mg^{2+} at 9:1 or 8:2) was reacted with the appropriate quantities of the acid solution to obtain a 100 ml total volume. The resulting solutions were then vigorously stirred into a slurry at 80 °C, and then dried in an oven at 70 °C for 12 h. After drying, the powder was calcined in a horizontal tube furnace at 800 °C for 2 h.

For comparison, a sorbent was also produced by the dry ball milling method, which involved combining an appropriate amount limestone and dolomite to achieve a molar ratio of Ca^{2+} to Mg^{2+} of 9:1. This material was then ground directly in a ball-grinder for 30 min and then calcined at 800 °C for 2 h. The ratios of organic acid per mole of CaO precursor for each sorbent are shown in Table 1.

The resulting sorbents were labelled using the following convention: the first part of the name referred to the precursor; L, D, or LD representing limestone, dolomite, or limestone and dolomite mixtures as the precursor, respectively. For the limestone and dolomite mixtures the number that follows refers to the molar ratio of Ca^{2+} to Mg^{2+} of 9:1 (LD9) and 8:2 (LD8). While, the second part of the naming convention identifies the type of organic acids, i.e. GA, CI, and AC represent the gluconic acid, citric acid, treated materials, respectively. BM represents the sorbents obtained by the ball milling treated method. As an example of the naming convention, LD9-GA represents the sorbent obtained from a mixed limestone and dolomite precursor using a molar ratio of Ca^{2+}:Mg^{2+} equal to 9:1 and reacted with gluconic

acid.

The sorbents without the organic acid and ball milling treatment were designated as LC and DC, and were obtained from the direct calcination of natural limestone or dolomite for comparison; again the calcination was performed at 800 °C for 2 h.

2.3 Characterization methods

The morphology of the fresh and cycled sorbents were characterized by scanning electron microscope at two different magnification ranges (SEM: JSM-6360LV). Simultaneously, an energy dispersive X-ray spectrometer (EDX: EDAX Genesis Apex 2 system) was used to compare the distribution of Ca^{2+} and Mg^{2+} ions over the structure of the sorbents. TGA (thermogravimetric analysis) and DTG (differential thermal gravimetric analysis) data for the uncalcined, gluconic acid treated, limestone/dolomite mixtures (the molar ratios of Ca to Mg fixed at 9:1) were obtained from a thermogravimetric analyzer (Netzsch STA449C) with a heating rate of 10 °C/min from room temperature to 1000 °C under air. The crystal phase composition of the samples was obtained by X-ray diffraction (XRD: Bruker Model D8 Advance) in the 2θ range of 10-90°. The specific surface area and pore properties of the sorbents were measured using Brunauer-Emmett-Teller N_2 adsorption-desorption isotherms (BET: Micromeritics ASAP-2010C).

2.4 CO_2 adsorption.

A thermogravimetric analyzer (ZRY-1P, Techcomp Jingke Scientific Instrument Co., Ltd., Shanghai, China) was used to study the cyclic carbonation and calcination characteristics of CO_2 sorbents. The following operating conditions were used in the

carbonation/calcination tests: carbonation was performed at 700 °C for 20 min in a 15 vol% CO_2 atmosphere, and the calcination phase was conducted at 950 °C for 5 min in a 100 vol% CO_2 atmosphere. The gas flow rate in all phases was maintained at 50 ml/min. The heating and cooling rates were 10 °C/min and 15 °C/min, respectively.

3. Results and Discussion

3.1 The cyclic CO_2 uptake capacity of L-GA or D-GA

The CO_2 uptake capacity was used to assess the cyclic activity of the prepared sorbents since the effect of inert MgO grains, present within the matrix of these dolomite derived sorbents, must be taken into account. The uptake capacity used here, is defined as the mass of CO_2 removed relative to the mass of sorbent before carbonation (which includes both CaO and MgO). The cyclic CO_2 uptake capacity of L-GA and D-GA (sorbents derived from gluconic acid treated limestone and dolomite), tested under realistic calcination conditions of 100% CO_2 and 950 °C, is plotted in Figure 1, and the uptake capacity results for the LC and DC (sorbents derived from limestone and dolomite) are also presented for comparison. Under realistic calcination conditions, DC gives a lower uptake capacity (0.42 g/g) relative to LC (0.63 g/g) during the initial cycles, but it deactivates with repeated cycling at a relatively slower rate when compared with the sorbent derived from limestone. Thus, the uptake capacity of DC (~0.40 g/g) is 1.6 times higher than that of LC (~0.25 g/g) after 10 cycles. Similar results have been previously reported [32], indicating that the sorbent obtained from dolomite has a higher residual uptake capacity than that from limestone, even when exposed to harsh calcination conditions.

To explore fundamental mechanisms responsible for the behavior of two natural CaO precursors, SEM images of both fresh and cycled sorbents have been obtained. As shown in Figure 2, by comparison with fresh LC (Figure 2a), the cycled LC (Figure 2b) exhibits significant sintering and has a compact and smooth surface. Such sintering leads to a sharp reduction of the reactive surface area, which agrees well with the drop in CO_2 uptake capacity observed in the TGA data. On the other hand, the DC sorbent (see the insets of Figure 2c-d) still shows a relatively high porosity, and hence a larger CO_2 capture capacity after 10 cycles. Note only slight sintering with an increase in grain size appeared on the surface of the cycled DC, which can be explained by the presence of MgO acting as a structural stabilizer. Previous work [31, 34] has shown that the MgO stabilizer should be mixed uniformly with active CaO to achieve favorable CO_2 uptakes over multiple cycles. Importantly, both MgO and CaO grains displayed homogeneous mixing in fresh DC. Nonetheless, MgO grains are clearly segregated on the surface of the cycled sample (Figure 2d), and this must therefore have had an effect on its cyclic uptake capacity. Taken, together with its relatively high stability in TGA results, it seems that the amount of stabilizer (the molar ratio of Ca^{2+} to Mg^{2+} is around 1:1) in cycled dolomite sorbent could have been reduced.

Turning to the cyclic CO_2 uptake capacity of L-GA and D-GA, both L-GA and D-GA showed an improved uptake in the first cycle (Figure 1a) as compared with LC or DC. This improvement is particularly noticeable in the case of L-GA, suggesting that gluconic acid treatment makes a significantly more effective contribution to the

sorbent obtained from limestone than dolomite. Previous studies[29, 41] using other types of acid for pretreatment found that treated limestone or dolomite sorbents demonstrated enhanced CO_2 capture performance during the initial cycles. However, with increasing number of cycles, L-GA suffers a drastic deactivation and its CO_2 uptake falls to around 0.30 g/g after 10 cycles. This value is just slightly higher than the residual uptake capacity of LC. For D-GA, a slight drop is observed with repeated cycling, and the decay behavior is comparable to the case of untreated DC sorbents. L-GA and D-GA exhibit similar cyclic CO_2 uptake characteristics to their respective untreated sorbent samples. In other words, under realistic carbonation/calcination conditions, the gluconic acid treatment step, on its own, does not seem to significantly improve the sorbents cyclic CO_2 capture performance. Miranda-Pizarro et al.[42] also reported similar results using acetic acid treated limestone and dolomite.

The microstructure of L-GA and D-GA before and after the multicycle tests was further analyzed by SEM, as shown in Figure 3. Compared with the untreated sorbents (Figures 2a and 2c), both treated sorbents (Figures 3a and 3c) exhibit a relatively porous sheet-like structure with small sized grains, leading to the increased CO_2 capture performance observed in the first cycle (Figure 1a). The sheets of the treated limestone sorbent were noticeably thinner and have a much higher visible porosity, which resulted in a significant improvement of its initial uptake of CO_2. After the 10 cycles, the cycled L-GA lost half of its CO_2 capture capacity, and the SEM imaging showed severe sintering of the CaO grains, as evidenced by the sorbent becoming more compact and shifting the general pore size towards larger pores that

are less useful for CO_2 capture. By contrast, the cycled D-GA shows even higher porosity than fresh sorbent despite its larger grain size, which explains why its capture capacity was maintained over 10 cycles. It also appears that the segregation of MgO grains of cycled D-GA was slightly mitigated compared with the case of cycled raw dolomite. Due to dolomite reacting with gluconic acid to form Ca-Mg gluconates with a more homogeneous mixture of Ca and Mg, the segregation of MgO in D-GA was reduced.

3.2 The cyclic CO_2 uptake capacity of LD9-GA and LD9-BM

Figure 1b compares multicycle uptake capacity of the sorbents using gluconic acid and dry ball-milling treatment with limestone/dolomite mixtures with molar ratios of Ca to Mg fixed at 9:1. With the ball-milling treatment, LD9-BM displayed a relatively high uptake capacity of 0.51 g/g in the 1st cycle. This value is higher than both cases of raw, untreated sorbents (LC and DC), and can be explained by a more favorable structure (i.e. a smaller particle size and greater surface area) for CO_2 capture induced by ball-milling and a reduced amount of inert MgO. Moreover, its deactivation rate is slower than LC but slightly higher than DC. The "improved" initial uptake capacity and deactivation rates are obviously different from the cases of the gluconic acid-treated sorbents and further indicate that a dry ball-milling treatment of limestone/dolomite mixtures clearly affects the cyclic CO_2 uptake characteristics of the raw sorbent, but this method fails to achieve the same cyclic stability as the sorbents derived from natural dolomite. Fortunately, the gluconic acid treated sorbent (LD9-GA) not only achieves an outstanding initial uptake capacity but also maintains

its high performance over multiple cycles. In the first cycle, its uptake capacity is 0.63 g/g, which is the largest among these sorbents, and this superior uptake is maintained over multiple cycles. Additionally, an increased uptake capacity is observed in the second cycle as a result of the phenomenon of "self-reactivation".[19, 20]

The effect of MgO content on the cyclic capture performance can be seen in Figure 1c, when the molar ratios of Ca to Mg decrease from 9:1 to 8:2, both of the two MgO-stabilized sorbents present a similar stable cyclic behavior, suggesting that increasing the MgO content beyond 10 mol% does not enhance the cyclic stability further. However, accompanied by this increase, the CO_2 uptake capacity decreases due to a reduction in the amount of active CaO, thus, the optimized MgO content appears to be no more than 10 mol%.

To explain the superior capture performance of LD9-GA, a series of characterizations of these materials were made. First, the thermograms (Figure 4) of uncalcined gluconic acid-reacted limestone/dolomite mixtures (LD9-GA) were examined by heating the samples from room temperature to 1000 °C at 10 °C/min under air. Based on the TGA and DTG curves, a three-step decomposition process is clearly observed. In the first step (around 5% mass loss), dehydration of the sorbent occurred at temperatures between 100 °C and 170 °C. The second mass loss (which represents approximately 79% of the total mass) took place from 180 °C to 520 °C, due to the decomposition of uncalcined limestone/dolomite and gluconic-acid mixtures into intermediate compounds ($CaCO_3$, MgO, CO_2, and acetone).[44, 45] Finally, the last mass loss (about 7%) began at ~700 °C and was complete by ~720 °C, and

this can be attributed to the decomposition of $CaCO_3$ to yield CaO. Similar to calcium gluconate derived CaO sorbents,[44, 45] the multi-step decomposition of gluconic-acid treated limestone/dolomite mixtures plays a critical role in the physico-chemical properties of CaO sorbents formed. Based on the TGA data, MgO-stabilized CaO sorbents were prepared following equation 2:

$$0.8\ CaCO_3 + 0.1\ CaMg(CO_3)_2 + 2\ C_6H_{12}O_7 \rightarrow Ca_{0.9}Mg_{0.1}C_{12}H_{22}O_{14} + CO_2 + H_2O$$

$$\rightarrow Ca_{0.9}Mg_{0.1}CO_3 \rightarrow Ca_{0.9}Mg_{0.1}O + CO_2 \quad (2)$$

The XRD patterns of four sorbents LC, DC, LD9-BM and LD9-GA is shown in Figure 5. LC shows the typical crystalline phase of CaO, and DC shows the typical crystalline peaks for CaO and MgO. No impurity phases for $CaCO_3$ or $CaMg(CO_3)_2$ were observed, suggesting that both limestone and dolomite were completely calcined. When treated by the ball-milling and gluconic acid, two phases of CaO and MgO were observed in the patterns of both treated sorbents, indicating that two treament process did not modify the chemical composition or crystalline phases present. The crystallite sizes of the sorbents were calculated using Scherrer's equation. The crystallite size of CaO (Table 2) in DC was found to be 69 nm, but the CaO crystallite size of LD9-BM was reduced to 45 nm from the treatment of the ball-milling. By contrast, a remarkably reduced CaO crystallite size for gluconic acid treatment (LD9-GA) was achieved, 38 nm; representing the smallest CaO crystallite size and this likely contributed to the greater reactivity in CO_2 capture process.

Subsequently, the N_2 absorption/desorption isotherms were used to compare the textures of LD9-BM and LD9-GA. As shown in Table 3, the specific surface area of

LD9-GA is 27.11 m^2/g, which was two times larger than the value for LM9-BM. In comparison with LD9-BM, LD9-GA also presents a more porous structure with a larger pore volume and broader pore-size distribution. According to Liu et al.,[44] a large amount of gas is generated during the decomposition of CaO precursors which results in an improved pore structure of CaO sorbent. Considering the remaining sample weight of ~10% (Figure 4), approximately 90% of the total mass loss during decomposition allows LD9-GA to exhibit more porous features, thus ensuring the improved diffusion of CO_2 to the inner CaO grains.

Finally, the SEM micrographs and EDX mapping were probed to compare the morphologies and compositional homogeneity of LD9-BM and LD9-GA. LD9-BM (see the inset of Figure 6a) appears to have a rather "fragile" morphology with a relatively wide particle size distribution (~1-4 μm) caused by inhomogeneous mixing of CaO and MgO during the mechanical ball-milling process. The high magnification for Figure 6a further reveals that tiny snowflake-like particles (MgO) have segregated form these micrometer-sized particles (CaO). EDX mapping (Figure 7a) also confirms an inhomogeneous distribution of MgO within the active CaO in LD9-BM. Due to its inhomogeneous composition, the cycled LD9-BM presented a comparatively sintered surface with segregated MgO particles (Figure 6b), in turn leading to a slight enhancement over the CO_2 uptake of LC. However, LD9-GA (Figure 6c) is significantly different from LD9-BM,and shows a considerably more uniform but loose nanosheet (~100 nm thick) morphology that is comprised of a homogeneous mix of CaO and MgO at the nanometer scale. EDX mapping (Figure 7b) also shows a

homogeneous distribution of MgO within the CaO matrix in LDM-GA, thereby demonstrating the cycled LDM-GA transformation into a multilayered structure with highly macroporous nano-skeletons. The close-up view of the skeleton showed that the compositional homogeneity was retained, since MgO and CaO particles are difficult to distinguish from each other even at the nanoscale. The microstructure analysis demonstrates that homogeneous mixing is not only seen in the fresh LD9-GA but also in its cycled sample, which is highly desirable for a structural stabilization and in turn, produces a high initial uptake capacity and cyclically stability.

3.3 The cyclic CO_2 uptake capacity of LD9-CI and LD9-AC

To validate the advantages of the acid treated approach in more detail, other acids (acetic acid and citric acid) were used to obtain MgO-stabilized sorbents (the molar ratios of Ca to Mg were all 9:1). Figure 1d illustrates the cyclic CO_2 uptake of MgO-stabilized sorbents derived from LD9 reacted with three types of acid. Both sorbents from acetic acid and citric acid treatment all demonstrated improved cyclic CO_2 uptakes when compared with LD9-BM. Moreover, their cyclic performances were found to be largely dependent of type of acid used in the pretreatment step. In comparison with LD9-GA (Figure 1b), LD9-CI presented a comparable initial uptake capacity, but it showed a relatively faster drop in reactivity with increasing cycle number. Among these sorbents, LD9-GA showed the highest CO_2 uptake and best cyclic stability, suggesting that the most efficient acid treatment was gluconic acid.

The influence of acid type on the multicycle activity is related to the physio-chemical properties of the formed CaO sorbents, which must be dependent on

the decomposition of the Ca-Mg mixed carbonates and gluconic acid. From the thermograms of gluconic acid-treated limestone/dolomite mixtures in Figure 4, this decomposition is similar to the case of calcium gluconate. According to previous studies[28, 45] involving organic acid treated limestone, the total mass reduction during decomposition can be ranked as follows: LD9-GA > LD9-CI > LD9-AC. Moreover, CaO crystallite size in LD9-GA was smaller than that of LD9-CI and LD9-AC.

Similar to fresh LD9-BM, the SEM images (Figure 8a) LD9-AC exhibited an irregular structure with comparatively large aggregated grains (>4 μm). The porosimetry analysis from N_2 adsorption (Table 3) reveals that the specific surface area, pore volume and average pore size of LD9-AC were slightly higher than those of LD9-BM. Cycled LD9-AC (Figure 8b) also presented a comparatively sintered morphology. The comparatively improved microstructure and porous texture confirm that LD9-AC demonstrated a slight enhancement in the CO_2 uptake of LD9-BM. For fresh LD9-CI, the presence of comparatively large aggregated grains disappeared and are replaced by twisted and separated filaments (Figure 8c), which also presented a more porous texture than that of LD9-AC as can be seen in Table 3. These favorable features contribute to its remarkably high initial CO_2 uptake capacity. However, in contrast to the case of LD9-GA, LD9-CI's high uptake capacity cannot be maintained due to the relatively severe sintering observed.

Here, the soluble gluconic acid treatment facilitated compositional homogeneity between MgO and CaO as no clear segregations were observed in both fresh and cycled samples (Figure 8). Furthermore, the high and cyclically stable CO_2 uptake

was not achieved by treating the same precursor materials with acetic or citric acid. These observations suggest that homogeneous mixing was not sufficient on its own to produce the superior capture performance, and instead the unique microstructure with macroporous nanosheet morphology (observed in LD9-GA) was required to provide enough void volume to allow for the volume expansion during carbonation and mitigating agglomeration and structural collapse. Conversely, due to the absence of enough void space in LD9-AC and LD9-CI, these particles tended to be sintered together into large and compact aggregates as observed in the SEM images of the cycled samples (Figures 8b and d).

3.4 The role of overall CaO conversion of LD9-GA during multicycles

From a fundamental perspective, besides the uptake capacity, another parameter that must be considered is the actual conversion of CaO in each cycle. Such CaO conversion is here defined as the ratio of mass of CaO converted in each carbonation regime to the initial mass of CaO in the sorbent. Figure 9a displays the time evolution of the overall CaO conversion for the first carbonation among three sorbents (LC, DC and LD9-GA). In general, the curves of the three sorbents all show that carbonation at 700 °C in 15% CO_2 proceeds through an initial fast reaction (FR)-controlled regime occurring on the surface of CaO and followed by a relatively slow diffusion (SD)-controlled regime due to the diffusion of CO_2 through the $CaCO_3$ product layer covering the CaO surface. When the set point temperature was increased to 950 °C in pure CO_2, carbonation continued to progress due to the “re-carbonation” (RE) regime. The boundary between these three regimes is also shown in Figure 9a.

The contributions of the FR, SD and RE regimes on the overall CaO conversion for these three sorbents over 10 cycles is shown in Figures 9b, c, and d, respectively. In FR regime (0-8.5min), the greatest CaO conversion among the three sorbents, after 10 cycles, was observed in LD9-GA, caused by its highly porous texture. This observation also indicates that LD9-GA may be promising in practical circulating fluidized bed reactors given their short residence times (on the order of several minutes). In the SD regime (8.5-20 min), the highest CaO conversion after 10 cycles was observed for LD9-GA, which can be ascribed to its smallest CaO crystallite size providing the path of least resistance for the CO_2 diffusion. With regards to the effect of RE, the CaO conversion of LD9-GA was as high as 90% with a negligible capacity decay during 10 cycles.

Compared with previously reported effective CaO precursors (Calcium Gluconate[44] ~2500 $/ton)), our procedure using gluconic acid (~820 $/ton) treated limestone/dolomite (~50+$/ton) is relatively cheap and simpler for practical application. Moreover, the cost could be further decreased optimizing the ratio of acid to Ca to reduce the amount of gluconic acid and using alternative biomass derivatives as a cost-effective resource for gluconic acid production. As regard to citric acid and acetic acid, they both have a fairly low price (~400 $/ton). A further techno-economic analysis will be carried out to determine the effect of possible acid consumption and limestone/dolomite sorption effectiveness in CaL. On the other hand, ensuring operability of sorbents in a scaled up reactor is vitally important for future commercialization efforts. Thus, the granulation and pelletisation of these materials

along with fluidized bed testing will be needed.

4 Conclusions

TGA results show that, individually, limestone and dolomite treated with gluconic acid (GA) does not inherently improve the cyclic capture performance under realistic carbonation/calcination cycles. Instead, microstructure characterizations indicate that cycled limestone treated with gluconic acid (L-GA) showed significant sintering due to the lack of a structural stabilizer. Similarly, dolomite treated with gluconic acid (D-GA) showed a clear segregation of MgO grains in after cycling and in turn lost their stabilizing role. Due to the inhomogeneous composition between CaO and MgO, a sample of mixed limestone and dolomite treated by ball milling (LD9-BM) exhibited a slightly enhanced cyclic uptake compared to that of limestone on its own (LC). Although samples of mixed limestone and dolomite treated with acetic (LD9-AC) and citric acid LD9-CI demonstrated compositional homogeneity, a high and stable CO_2 uptake did not result and instead the sorbents were found to agglomerate and suffer from structural collapse, which appears to be due to a lack of enough void space for the volume expansion during carbonation. However, a sample of mixed limestone and dolomite treated with gluconic acid (LD9-GA) did present a homogeneous mixture of CaO and MgO as a porous MgO-stabilized CaO nanosheet (~100 nm thick). This sorbent was able to provide enough void space for the volume expansion during carbonation to mitigate sintering and retain structural stabilization. Thus, a MgO content as low as 10 mol% was found to be sufficient to retain a CO_2 uptake of 0.60 g/g after 10 cycles under realistic carbonation/calcination conditions.

In particular, the CaO conversion of LD9-GA was as high as 90% with a negligible CO_2 capture capacity loss over 10 reaction cycles when a recarbonation process was employed.

Acknowledgement

This work was supported by financial supports from the Fundamental Research Funds for the Central Universities (2018XKQYMS13).

References

(1) Rhodes, C. J., The 2015 Paris Climate Change Conference: COP21. *Sci. Prog.* **2016,** 99 (1), 97-104.

(2) Bui, M.; Adjiman, C. S.; Bardow, A.; Anthony, E. J.; Boston, A.; Brown, S.; Fennell, P. S.; Fuss, S.; Galindo, A.; Hackett, L. A.; Hallett, J. P.; Herzog, H. J.; Jackson, G.; Kemper, J.; Krevor, S.; Maitland, G. C.; Matuszewski, M.; Metcalfe, I. S.; Petit, C.; Puxty, G.; Reimer, J.; Reiner, D. M.; Rubin, E. S.; Scott, S. A.; Shah, N.; Smit, B.; Trusler, J. P. M.; Webley, P.; Wilcox, J.; Mac Dowell, N., Carbon capture and storage (CCS): the way forward. *Energy Environ. Sci.* **2018,** 11 (5), 1062-1176.

(3) Erans, M.; Manovic, V.; Anthony, E. J., Calcium looping sorbents for CO_2 capture. *Appl. Energy* **2016,** 180, 722-742.

(4) Liu, W.; An, H.; Qin, C.; Yin, J.; Wang, G.; Feng, B.; Xu, M., Performance Enhancement of Calcium Oxide Sorbents for Cyclic CO_2 Capture-A Review. *Energy Fuels* **2012,** 26 (5), 2751-2767.

(5) Blamey, J.; Anthony, E. J.; Wang, J.; Fennell, P. S., The calcium looping cycle for large-scale CO_2 capture. *Prog. Energy Combust. Sci.* **2010,** 36 (2), 260-279.

(6) Perejon, A.; Romeo, L. M.; Lara, Y.; Lisbona, P.; Martinez, A.; Manuel Valverde, J., The Calcium-Looping technology for CO_2 capture: On the important roles of energy integration and sorbent behavior. *Appl. Energy* **2016,** 162, 787-807.

(7) Anthony, E. J., Ca looping technology: current status, developments and future directions. *Greenhouse Gases-Science and Technology* **2011,** 1 (1), 36-47.

(8) Strohle, J.; Junk, M.; Kremer, J.; Galloy, A.; Epple, B., Carbonate looping experiments in a 1 MWth pilot plant and model validation. *Fuel* **2014,** 127, 13-22.

(9) Arias, B.; Diego, M. E.; Abanades, J. C.; Lorenzo, M.; Diaz, L.; Martínez, D.; Alvarez, J.; Sánchez-Biezma, A., Demonstration of steady state CO_2 capture in a 1.7 MWth calcium looping pilot. *Int. J. Greenhouse Gas Control* **2013,** 18, 237-245.

(10) Hanak, D. P.; Anthony, E. J.; Manovic, V., A review of developments in pilot-plant testing and modelling of calcium looping process for CO_2 capture from power generation systems. *Energy Environ. Sci.* **2015,** 8 (8), 2199-2249.

(11) Coppola, A.; Scala, F.; Salatino, P.; Montagnaro, F., Fluidized bed calcium looping cycles for CO_2 capture under oxy-firing calcination conditions: Part 1. Assessment of six limestones. *Chem. Eng. J.* **2013,** 231, 537-543.

(12) Coppola, A.; Scala, F.; Salatino, P.; Montagnaro, F., Fluidized bed calcium looping cycles for CO_2

capture under oxy-firing calcination conditions: Part 2. Assessment of dolomite vs. limestone. *Chem. Eng. J.* **2013,** 231, 544-549.

(13) Valverde, J. M.; Sanchez-Jimenez, P. E.; Perez-Maqueda, L. A., Limestone Calcination Nearby Equilibrium: Kinetics, CaO Crystal Structure, Sintering and Reactivity. *J. Phys. Chem. C* **2015,** 119 (4), 1623-1641.

(14) Alvarez, D.; Pena, M.; Borrego, A. G., Behavior of different calcium-based sorbents in a calcination/carbonation cycle for CO_2 capture. *Energy Fuels* **2007,** 21 (3), 1534-1542.

(15) Manovic, V.; Charland, J.-P.; Blamey, J.; Fennell, P. S.; Lu, D. Y.; Anthony, E. J., Influence of calcination conditions on carrying capacity of CaO-based sorbent in CO_2 looping cycles. *Fuel* **2009,** 88 (10), 1893-1900.

(16) Manovic, V.; Anthony, E. J., Sintering and Formation of a Nonporous Carbonate Shell at the Surface of CaO-Based Sorbent Particles during CO_2-Capture Cycles. *Energy Fuels* **2010,** 24 (10), 5790-5796.

(17) Wang, K.; Guo, X.; Zhao, P. F.; Zhang, L. Q.; Zheng, C. G., CO_2 capture of limestone modified by hydration-dehydration technology for carbonation/calcination looping. *Chem. Eng. J.* **2011,** 173 (1), 158-163.

(18) Martinez, I.; Grasa, G.; Murillo, R.; Arias, B.; Abanades, J. C., Evaluation of CO_2 Carrying Capacity of Reactivated CaO by Hydration. *Energy Fuels* **2011,** 25 (3), 1294-1301.

(19) Manovic, V.; Anthony, E. J., Thermal Activation of CaO-Based Sorbent and Self-Reactivation during CO_2 Capture Looping Cycles. *Environ. Sci. Technol.* **2008,** 42 (11), 4170-4174.

(20) Lan, P.; Wu, S., Mechanism for self-reactivation of nano-CaO-based CO_2 sorbent in calcium looping. *Fuel* **2015,** 143, 9-15.

(21) Valverde, J. M.; Sanchez-Jimenez, P. E.; Perez-Maqueda, L. A.; Quintanilla, M. A. S.; Perez-Vaquero, J., Role of crystal structure on CO_2 capture by limestone derived CaO subjected to carbonation/recarbonation/calcination cycles at Ca-looping conditions. *Appl. Energy* **2014,** 125, 264-275.

(22) Arias, B.; Grasa, G. S.; Alonso, M.; Abanades, J. C., Post-combustion calcium looping process with a highly stable sorbent activity by recarbonation. *Energy Environ. Sci.* **2012,** 5 (6), 7353-7359.

(23) González, B.; Blamey, J.; Al-Jeboori, M. J.; Florin, N. H.; Clough, P. T.; Fennell, P. S., Additive effects of steam addition and HBr doping for CaO-based sorbents for CO_2 capture. *Chem. Eng. Process.* **2016,** 103, 21-26.

(24) Duan, L.; Su, C.; Erans, M.; Li, Y.; Anthony, E. J.; Chen, H., CO_2 Capture Performance Using Biomass-Templated Cement Supported Limestone Pellets. *Ind. Eng. Chem. Res.* **2016,** 55 (39), 10294-10300.

(25) Erans, M.; Cerciello, F.; Coppola, A.; Senneca, O.; Scala, F.; Manovic, V.; Anthony, E. J., Fragmentation of biomass-templated CaO-based pellets. *Fuel* **2017,** 187, 388-397.

(26) Sun, J.; Liu, W.; Chen, H.; Zhang, Y.; Hu, Y.; Wang, W.; Li, X.; Xu, M., Stabilized CO_2 capture performance of extruded-spheronized CaO-based pellets by microalgae templating. *Proc. Combust. Inst.* **2017,** 36 (3), 3977-3984.

(27) Xu, Y.; Ding, H.; Luo, C.; Zheng, Y.; Xu, Y.; Li, X.; Zhang, Z.; Shen, C.; Zhang, L., Effect of lignin, cellulose and hemicellulose on calcium looping behavior of CaO-based sorbents derived from extrusion-spherization method. *Chem. Eng. J.* **2018,** 334, 2520-2529.

(28) Hu, Y.; Liu, W.; Sun, J.; Li, M.; Yang, X.; Zhang, Y.; Liu, X.; Xu, M., Structurally improved CaO-based sorbent by organic acids for high temperature CO_2 capture. *Fuel* **2016,** 167, 17-24.

(29) Li, Y.j.; Zhao, C.s.; Duan, L.b.; Liang, C.; Li, Q.z.; Zhou, W.; Chen, H.c., Cyclic calcination/carbonation looping of dolomite modified with acetic acid for CO_2 capture. *Fuel Process. Technol.* **2008,** 89 (12), 1461-1469.
(30) Antzara, A.; Heracleous, E.; Lemonidou, A. A., Improving the stability of synthetic CaO-based CO_2 sorbents by structural promoters. *Appl. Energy* **2015,** 156, 331-343.
(31) Naeem, M. A.; Armutlulu, A.; Imtiaz, Q.; Donat, F.; Schäublin, R.; Kierzkowska, A.; Müller, C. R., Optimization of the structural characteristics of CaO and its effective stabilization yield high-capacity CO_2 sorbents. *Nature Communications* **2018,** 9 (1), 2408.
(32) Valverde, J. M.; Sanchez-Jimenez, P. E.; Perez-Maqueda, L. A., Ca-looping for postcombustion CO_2 capture: A comparative analysis on the performances of dolomite and limestone. *Appl. Energy* **2015,** 138 (0), 202-215.
(33) Herce, C.; Stendardo, S.; Cortes, C., Increasing CO_2 carrying capacity of dolomite by means of thermal stabilization by triggered calcination. *Chem. Eng. J.* **2015,** 262, 18-28.
(34) Filitz, R.; Kierzkowska, A. M.; Broda, M.; Mueller, C. R., Highly Efficient CO_2 Sorbents: Development of Synthetic, Calcium-Rich Dolomites. *Environ. Sci. Technol.* **2012,** 46 (1), 559-565.
(35) Kierzkowska, A. M.; Pacciani, R.; Müller, C. R., CaO-Based CO_2 Sorbents: From Fundamentals to the Development of New, Highly Effective Materials. *ChemSusChem* **2013,** 6 (7), 1130-1148.
(36) Wang, K.; Yin, Z.; Zhao, P.; Han, D.; Hu, X.; Zhang, G., Effect of Chemical and Physical Treatments on the Properties of a Dolomite Used in Ca Looping. *Energy Fuels* **2015,** 29 (7), 4428-4435.
(37) Sánchez-Jiménez, P. E.; Valverde, J. M.; Perejón, A.; de la Calle, A.; Medina, S.; Pérez-Maqueda, L. A., Influence of Ball Milling on CaO Crystal Growth During Limestone and Dolomite Calcination: Effect on CO_2 Capture at Calcium Looping Conditions. *Crystal Growth & Design* **2016,** 16 (12), 7025-7036.
(38) Sayyah, M.; Lu, Y. Q.; Masel, R. I.; Suslick, K. S., Mechanical Activation of CaO-Based Adsorbents for CO_2 Capture. *Chemsuschem* **2013,** 6 (1), 193-198.
(39) Kurlov, A.; Broda, M.; Hosseini, D.; Mitchell, S. J.; Pérez-Ramírez, J.; Müller, C. R., Mechanochemically Activated, Calcium Oxide-Based, Magnesium Oxide-Stabilized Carbon Dioxide Sorbents. *ChemSusChem* **2016,** 9 (17), 2380-2390.
(40) Sun, J.; Yang, Y.; Guo, Y.; Xu, Y.; Li, W.; Zhao, C.; Liu, W.; Lu, P., Stabilized CO_2 capture performance of wet mechanically activated dolomite. *Fuel* **2018,** 222, 334-342.
(41) Wang, K.; Hu, X.; Zhao, P.; Yin, Z., Natural dolomite modified with carbon coating for cyclic high-temperature CO_2 capture. *Appl. Energy* **2016,** 165, 14-21.
(42) Miranda-Pizarro, J.; Perejón, A.; Valverde, J. M.; Pérez-Maqueda, L. A.; Sánchez-Jiménez, P. E., CO_2 capture performance of Ca-Mg acetates at realistic Calcium Looping conditions. *Fuel* **2017,** 196, 497-507.
(43) Clough, P. T.; Boot-Handford, M. E.; Zhao, M.; Fennell, P. S., Degradation study of a novel polymorphic sorbent under realistic post-combustion conditions. *Fuel* **2016,** 186, 708-713.
(44) Zhao, P.; Sun, J.; Li, Y.; Wang, K.; Yin, Z.; Zhou, Z.; Su, Z., Synthesis of Efficient CaO Sorbents for CO_2 Capture Using a Simple Organometallic Calcium-Based Carbon Template Route. *Energy Fuels* **2016,** 30 (9), 7543-7550.
(45) Liu, W.; Low, N. W. L.; Feng, B.; Wang, G.; Diniz da Costa, J. C., Calcium Precursors for the Production of CaO Sorbents for Multicycle CO_2 Capture. *Environ. Sci. Technol.* **2009,** 44 (2), 841-847.

Table 1. Details of the prepared sorbents.

CaO precursor	Modification	Molar ratios (Ca:Mg: Acid)	Sorbent name
limestone	gluconic acid	1:3.5	L-GA
dolomite	gluconic acid	1:9.6	D-GA
limestone-dolomite mixtures	gluconic acid	9:1:38.2	LD9-GA
limestone-dolomite mixtures	gluconic acid	8:2:59.6	LD8-GA
limestone-dolomite mixtures	acetic acid	9:1: 398.6	LD9-AC
limestone-dolomite mixtures	citric acid	9:1:12	LD9-CI
limestone-dolomite mixtures	ball milling	9:1	LD9-BM
limestone	direct calcination	--	LC
dolomite	direct calcination	--	DC

Table 2. The crystal sizes of CaO calculated by Scherrer equation

Sample	DC	LD9-BM	LD9-GA
Particle size (nm)	69	45	38

Table 3. Pore properties of different prepared sorbents

Sample	Surface area (m^2/g)	Pore volume (cc/g)	Average pore diameter (nm)
LD9-BM	10.08	0.05	23
LD9-GA	27.11	0.19	34
LD9-AC	15.49	0.15	38
LD9-CI	16.03	0.12	29

Figure 1. CO_2 capture performance of sorbents in 10 cycles. (a) CaO sorbents from gluconic acid treated limestone and dolomite. (b) CaO sorbents from dry ball-milling and gluconic acid treated limestone/dolomite mixtures. (c) CaO sorbents from gluconic acid treated limestone/dolomite mixtures with different mole ratio of Ca/Mg. (d) CaO sorbents from different acid treated limestone/dolomite mixtures. GA, CI, and AC represent the gluconic acid, citric acid, and acetic acid treatment methods, respectively. BM represents the sorbents obtained by the ball milling modification method.

Figure 2. SEM image of the limestone or dolomite sorbents. (a) Fresh LC. (b) Cycled LC after 10 cycles. (c) Fresh DC. (d) Cycled DC after 10 cycles.

Figure 3. SEM image of the sorbents from the gluconic acid treated limestone or dolomite. (a) Fresh L-GA. (b) Cycled L-GA after 10 cycles. (c) Fresh D-GA. (d)

Cycled D-GA after 10 cycles.

Figure 4. The thermograms of uncalcined gluconic acid-treated limestone/dolomite mixtures in the synthesis of LD9-GA.

Figure 5. The XRD patterns of four sorbents

Figure 6. The SEM micrographs. (a) Fresh sample of LD9-BM. (b) Cycled of LD9-BM after 10 cycles. (c) Fresh LD9-GA. (d) Cycled of LD9-GA after 10 cycles.

Figure 7. EDX mapping. (a) and (b) Fresh LD9-BM. (c) and (d) Fresh LD9-GA. Purple and blue dots represent Ca and Mg.

Figure 8. SEM image of samples after different acid treatment. (a) Fresh sample of LDM-AC. (b) The cycled of LDM-AC. (c) Fresh sample of LDM-CI. (d) The cycled of LDM-CI.

Figure 9. Conversion of CaO for three sorbents in three different stages. (a) Typical time evolution of the overall CaO conversion in the first carbonation process. (b) After fast reaction (FR) regime. (c) After slow diffusion regime. (d) After re-carbonation (RE) regime during 10 cycles.

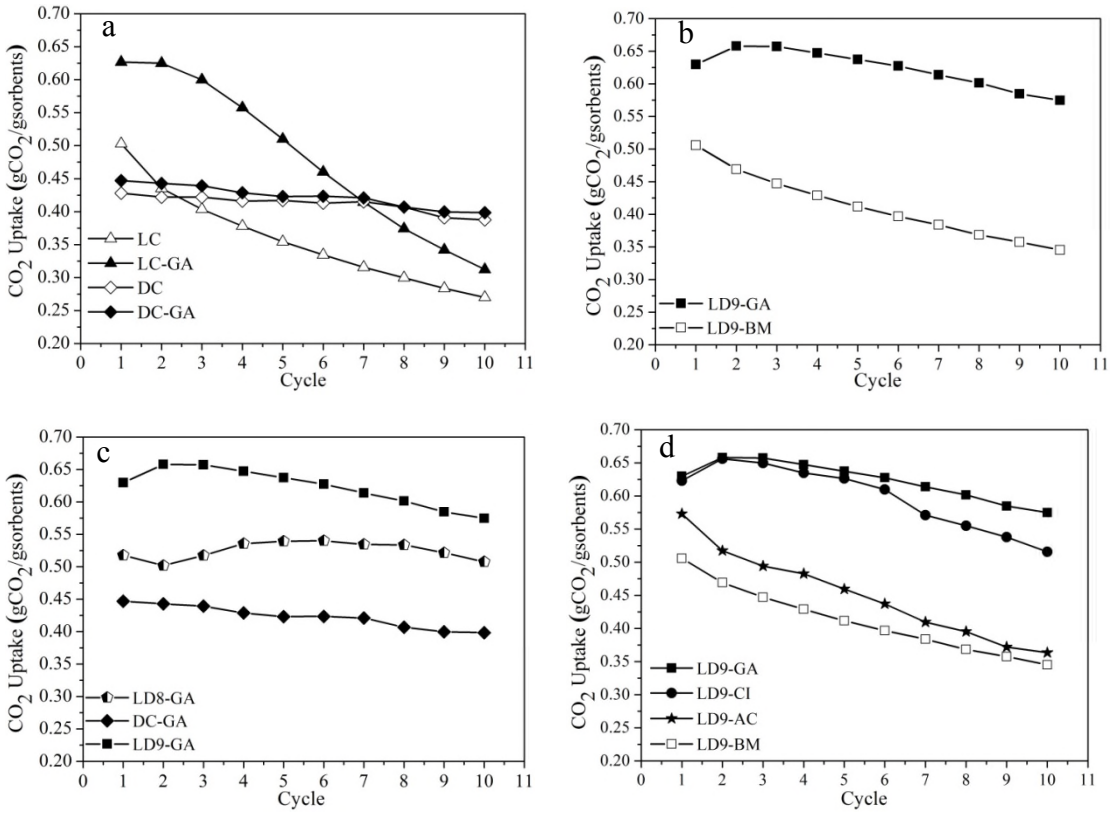
a
b
c
d
CO2 Uptake (gCO2/gsorbents)
Cycle
LC
LC-GA
DC
DC-GA
LD9-GA
LD9-BM
LD8-GA
LD9-CI
LD9-AC

Figure 1.

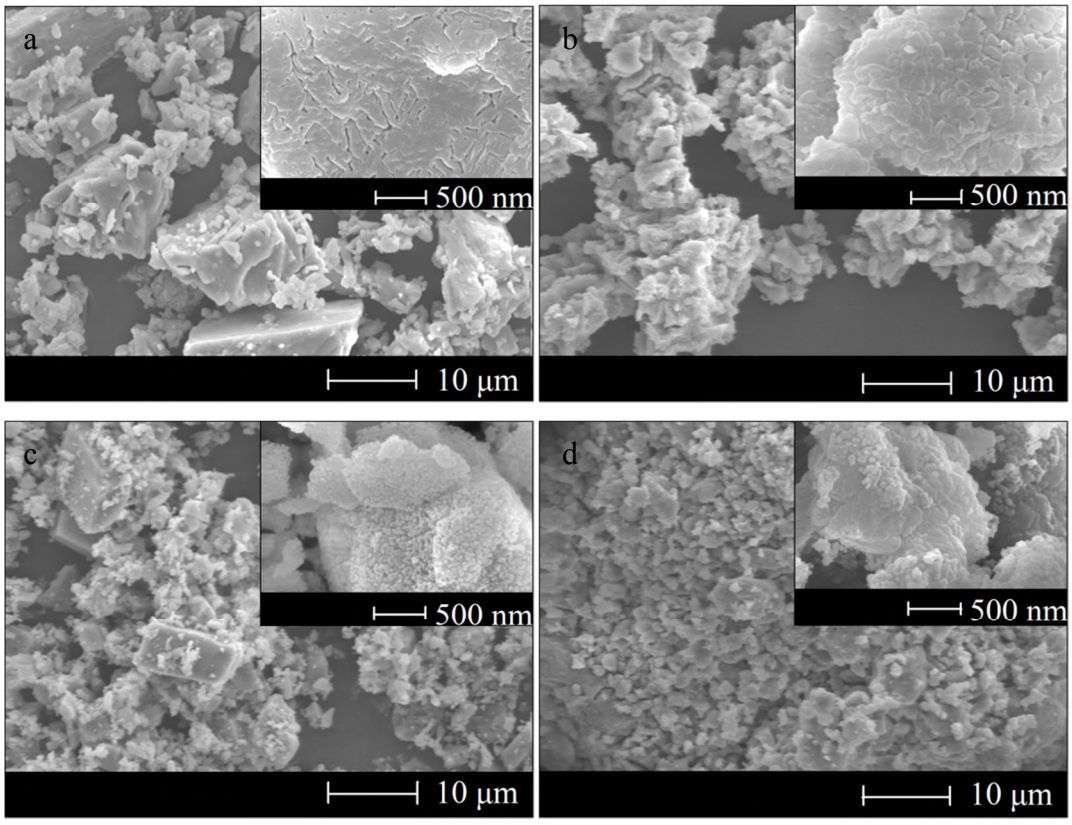

Figure 2.

.

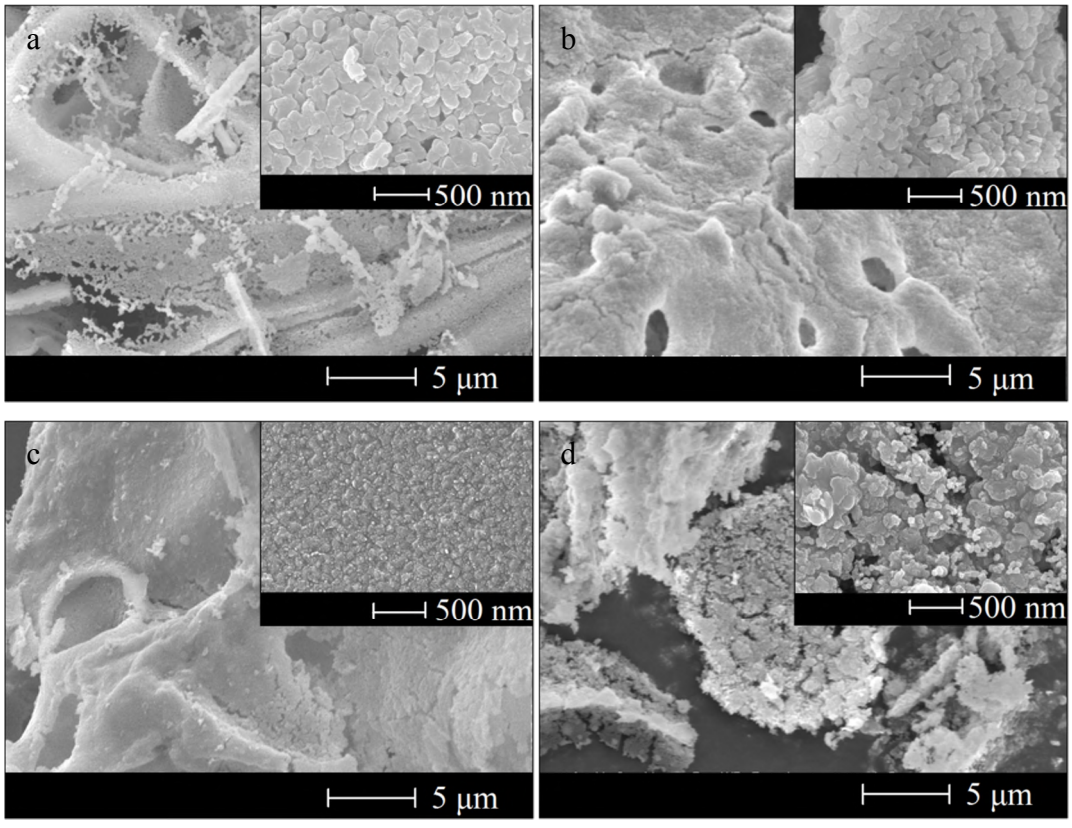

Figure 3.

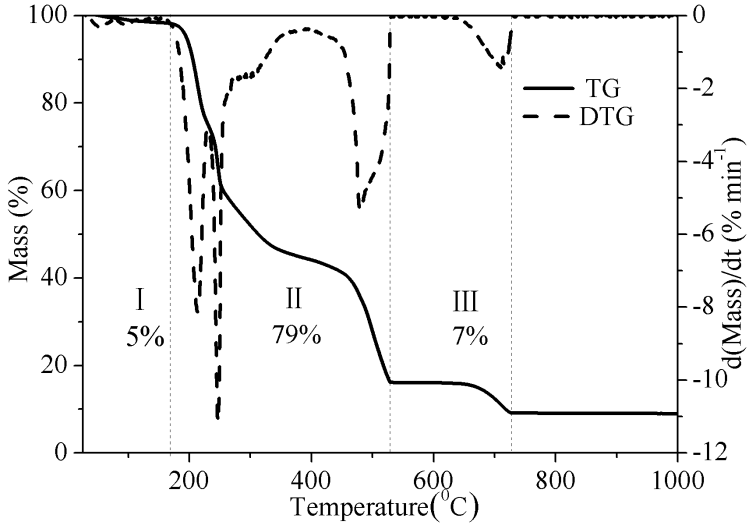
100
80
60
40
20
0
Mass (%)
0
-2
-4
-6
-8
-10
-12
d(Mass)/dt (% min-1)
TG
DTG
I
5%
II
79%
III
7%
200
400
600
800
1000
Temperature(0C)

Figure 4.

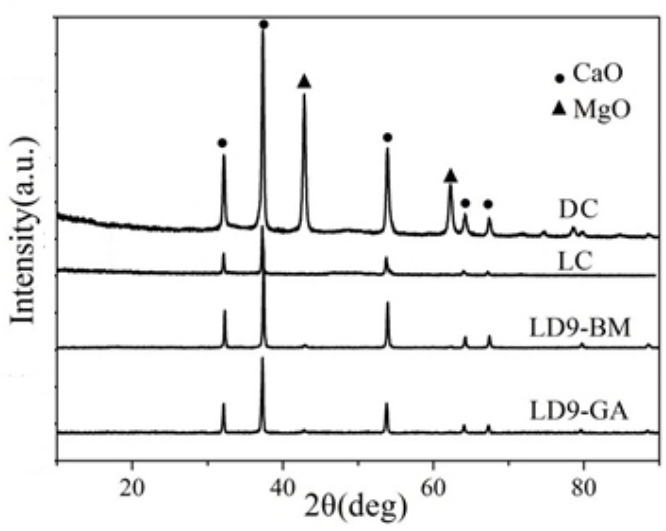

Figure 5.

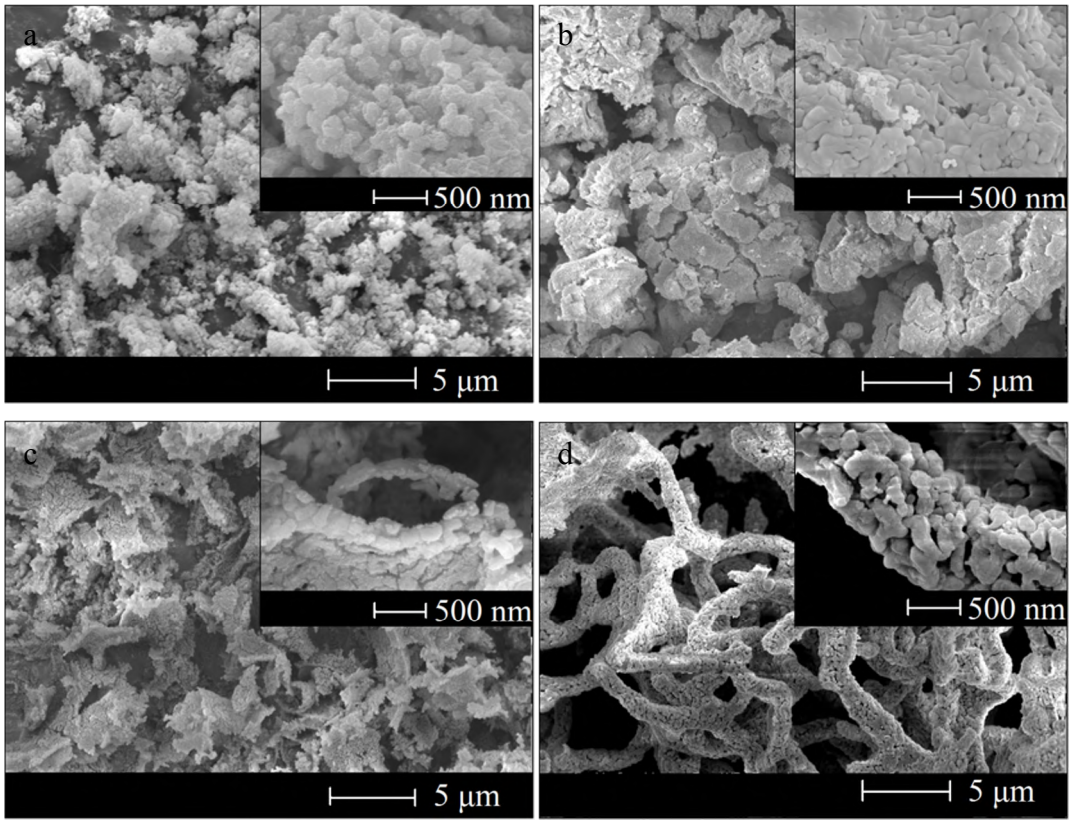

Figure 6.

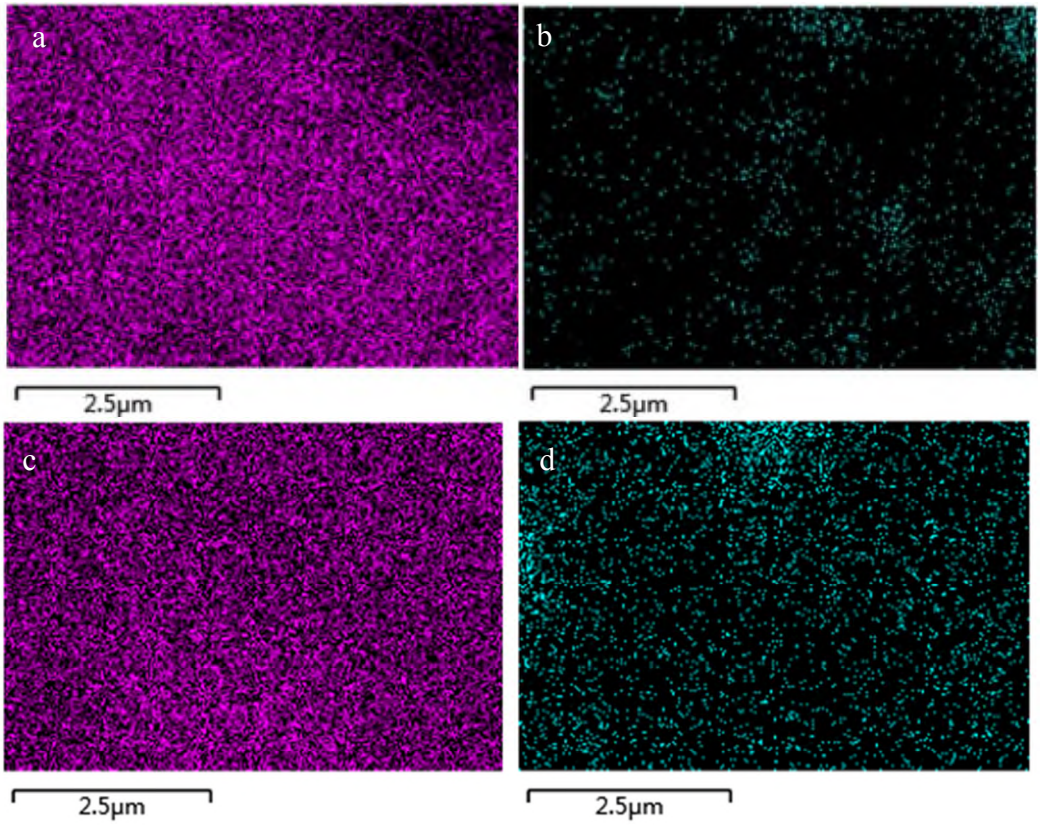

Figure 7.

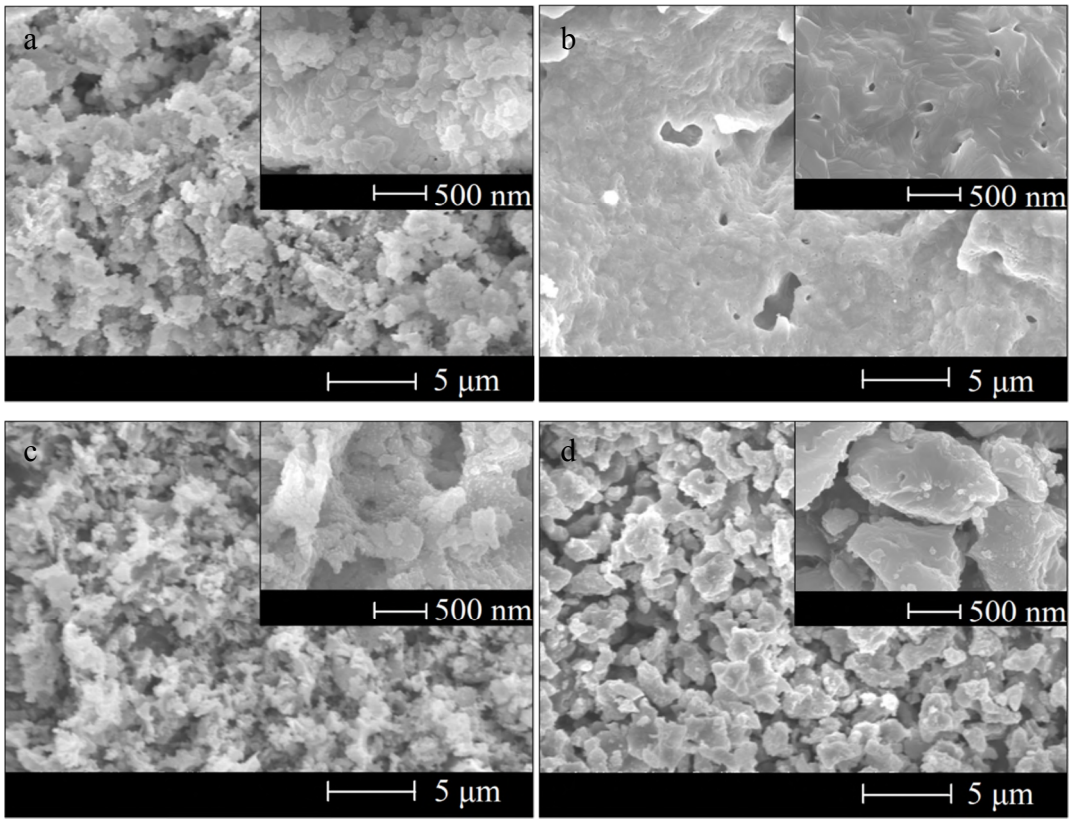

Figure 8.

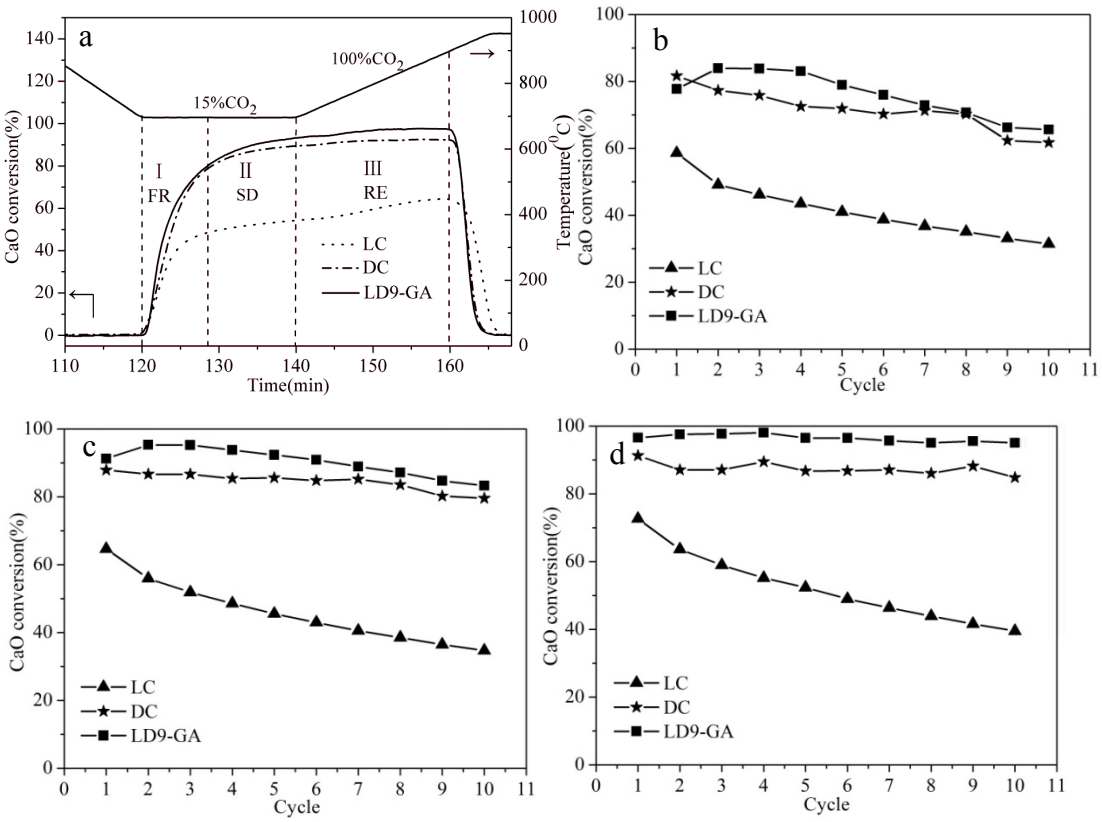
a
100%CO2
15%CO2
I
FR
II
SD
III
RE
LC
DC
LD9-GA
CaO conversion(%)
Temperature(0C)
Time(min)
b
CaO conversion(%)
Cycle
LC
DC
LD9-GA
c
CaO conversion(%)
Cycle
LC
DC
LD9-GA
d
CaO conversion(%)
Cycle
LC
DC
LD9-GA

Figure 9.